ADVANCED PHOTOVOLTAIC POWER SYSTEMS USING TANDEM GaAs/GaSb CONCENTRATOR MODULES

**L. M. Fraas, M. S. Kuryla, D. A. Pietila,
V. S. Sundaram, P. E. Gruenbaum, J. E. Avery,
V. Dinh, R. Ballantyne, and C. Samuel**

Boeing High Technology Center

Abstract

In 1989, Boeing announced the fabrication of a tandem gallium concentrator solar cell with an energy conversion efficiency of 30%. This research breakthrough has now led to panels which are significantly smaller, lighter, more radiation resistant, and potentially less expensive than the traditional silicon flat plate electric power supply.

The new Boeing tandem concentrator (BTC) module uses an array of lightweight silicone Fresnel lenses mounted on the front side of a light weight aluminum honeycomb structure to focus sunlight onto small area solar cells mounted on a thin back plane. This module design is shown schematically in *Figure 3*.

The tandem solar cell in this new module consists of a gallium arsenide light sensitive cell with a 24% energy conversion efficiency stacked on top of a gallium antimonide infrared sensitive cell with a conversion efficiency of 6%. This gives a total efficiency 30% for the cell-stack. The lens optical efficiency is typically 85%. Discounting for efficiency losses associated with lens packing, cell wiring and cell operating temperature still allows for a module efficiency of 22% which leads to a module power density of 300 Watts/m2. This performance provides more than twice the power density available from a single crystal silicon flat plate module and at least four times the power density available from amorphous silicon modules.

The fact that the lenses are only 0.010" thick and the aluminum foil back plane is only 0.003" thick leads to a very lightweight module. Although the cells are an easy to handle thickness of 0.020", the fact that they are small, occupying one-twenty-fifth of the module area, means that they add little to the module weight. After summing all the module weights and given the high module power, we find that we are able to fabricate BTC modules with specific power of 100 watts/kg.

An additional salient strength of these new BTC modules is their radiation resistance. This resistance arises not simply from the use of GaAs cells but perhaps more importantly from the use of thicker protective cover slides. Since the cells are small, thick cover slides can be used to protect the cells without adding appreciably to the module weight.

Finally, although the Boeing breakthrough announcement in 1989 emphasized performance improvements, the use of a sunlight concentrating lens array also promises major economic advantages. The concentrator approach substitutes easily molded inexpensive silicone Fresnel lenses for expensive single crystal semiconductor material. For example, one 4" diameter GaAs wafer will supply all the cells required to fabricate one 12 lens by 12 lens (18" by 18") BTC module. Furthermore, the 144 small concentrator cells obtained from this one wafer are easily fabricated and manipulated with high yield and without breakage. Contrast the cost of fabrication of the 121 thin (0.006") large area (1.58" by 1.58") GaAs cells required to make an equivalent area, lower power flat plate GaAs module and one can readily see the potential economic advantage of the BTC concept.

While the tandem-cell-stack efficiency values are impressive, the commercial commodity will be a power module integrating these cell-stacks. The recent focus of our efforts has been to demonstrate that concentrator power modules using tandem-cell-stacks can be easily assembled with automated equipment to produce high performance at low cost.

In the first section of this paper, we describe two types of cell-stack assembly processes. The first is the original wire-bonding technology that has been used in several of our modules. The second is a tape automated bonding (TAB) technology that we have developed for automated packaging. In the second section of this paper, we describe the assembly, testing, and performance of rugged concentrator minimodules designed for performance verification and as reference standards used to measure larger production modules.

Tandem Cell-Stack Assembly

A. Wire-bonded Cell Stacks

Boeing has fabricated the photovoltaic advanced space power (PASP) test-flight module[8] shown in *Figure 1*. This PASP module served as a vehicle for environmental testing done in collaboration with NASA and will be launched by the US Air Force in the fall of 1992 on a test mission to prove the viability of the technology. Although this module has achieved several of our initial goals, it is still only a test module, not a production module. This flight test module is significantly smaller than the proposed production module and it was assembled largely by hand. In particular, the cell-stacks were interconnected with copper wire soldered between stacks rather than flex circuit interconnects.

Figure 2 shows a sketch of a cell-stack typical of those used on the PASP flight-test module. A GaSb cell is first die bonded onto a metalized ceramic heat spreader with a separate metal pad forming the electrical contact to the back of the cell. Wire bond connections are then made from the top of the GaSb cell to a second metal pad on the ceramic. Then, silicone rubber spacers are formed on the corners of the GaSb cell and the GaAs top cell is then bonded in place on top of the GaSb cell. Although not shown, the ends of ribbons previously bonded to the back of the GaAs cell are then bonded down to a third metal pad on the ceramic. Finally, wire bond connections are made from the top of the GaAs cell to a fourth metal pad on the ceramic. The attachment of a cover slide is then optional at this point. The above sequence is actually done in batches of nine cells a pre-scribed 2" x 2" alumina substrate with a 3 x 3 array of cell sites. Individual cell-stack assemblies are then obtained by breaking up the ceramic substrate. This cell stack has two important attributes: first, the cell-stacks are testable before module wiring, and second, this approach uses hybrid circuit board technology and equipment available at Boeing. It is quite suitable for small numbers of parts, but unfortunately it is very tedious for the production of the large numbers of parts that would be needed for a full array.

B. TAB cell stacks

Figure 3 shows a drawing of our proposed production module assembly concept. For clarity, this figure shows a representative 4 by 6 lens/cell array. A production module would contain a larger number of array elements. The key assembly concepts shown in this figure are: (1) a prefabricated lens parquet; (2) cell-stacks interconnected through a prefabricated flex circuit mounted on the front surface of the panel back plane; and (3) pretested cell-stacks excised from TAB tape and inserted onto the flex circuit cell sites.

Figure 4 shows schematically a TAB process for the production of testable cell-stacks. In this TAB process, the spacers on the GaSb chips are applied at the wafer level by photolithography or screen printing (see *Figure 5*). As the two types of wafers are diced up, die of each type are glued together to create cell-stacks. These cell-stacks are then inner lead bonded into a three-beam-set TAB tape. These lead sets contact the top and bottom of the top cell and the top of the bottom cell. The stack can then be tested in the tape by probing pads on the tape and the bottom of the bottom cell.

The above stack production process begins with the adhesive bonding of the two types of chips to form the cell-stack. There are three requirements imposed at this point: first, the bond line must be very thin for good heat transport from the top chip through to the bottom chip; second, this bond should maintain electrical isolation between the two cells; and third, the TAB bonding surfaces on the cells have to be maintained free of contamination. These three requirements are met using the spacer/dam concept shown in *Figure 5*. The 8 μm thick polyimide spacer/dam pattern shown is formed on each GaSb cell at the wafer level before testing and dicing. After testing and dicing, yielded GaSb chips are placed in an alignment jig as shown in *Figure 6a*. A pneumatic dispensing system is then used to apply a 230 $\pm$ 30 nl drop of optical adhesive at the center of each GaSb cell. Then the GaAs chips are placed onto the GaSb chips in the alignment jig as shown in *Figure 6b*. The adhesive flows outward as shown in *Figure 5*. The alignment plate containing multiple cell sites

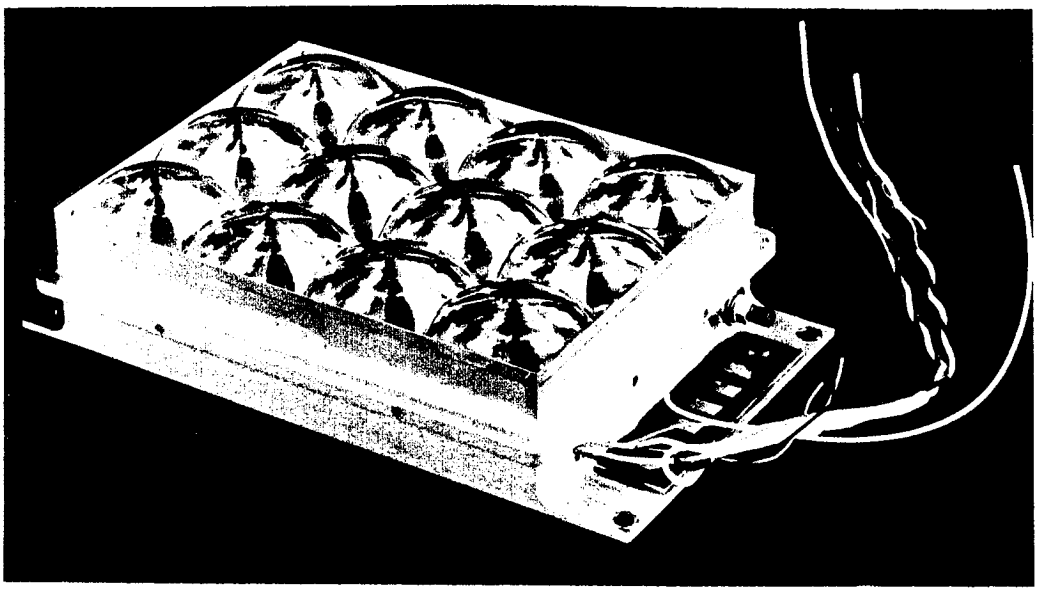

Fig. 1: Photograph of 12 lens concentrator module fabricated by Boeing for Photovoltaic Array Space Power Plus Diagnostics (PASP PLUS) flight experiment.

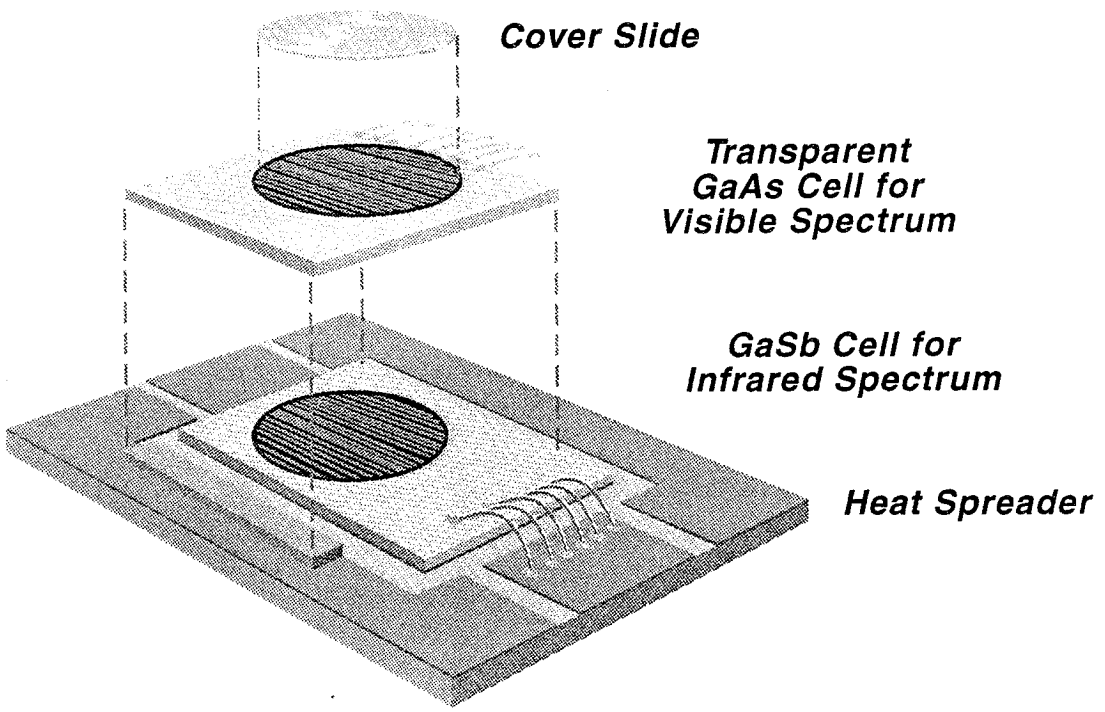

Fig. 2: GaAs/GaSb cell-stack in wire bonded form on ceramic substrate.

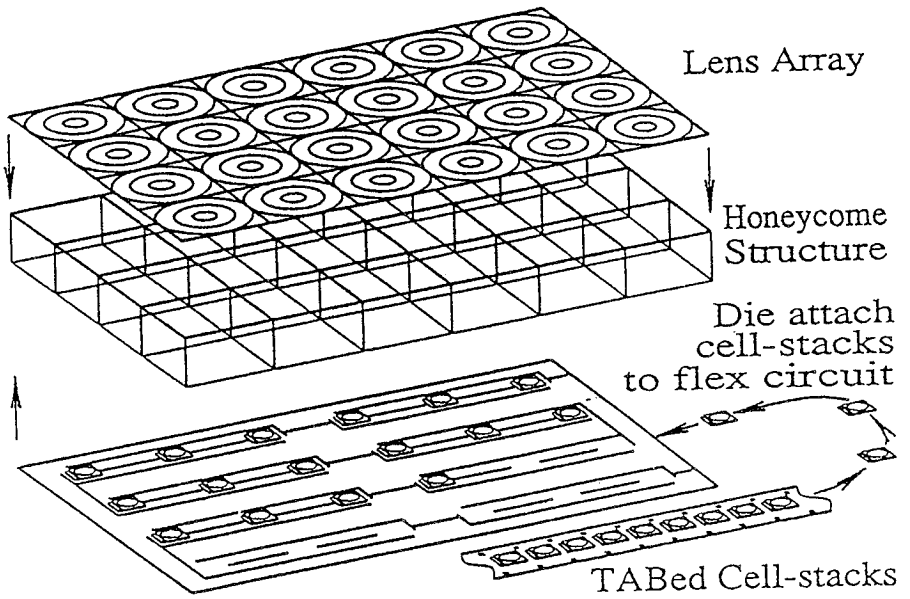

Fig. 3 A manufacturable tandem-cell concentrator module is shown schematically: consisting of a lens array, a honeycome housing, and an array of TABed cell-stacks bonded to a flex circuit on the module back plane.

is then heated to cure the adhesive. The resulting structures are aligned cell-stacks with uniform 8 μm thick bond lines. Adhesive is kept away from the TAB bond areas by the dams shown in *Figure 5*. Chiang and Gee have calculated that the temperature drop across a 12.5 μm thick RTV adhesive bond line will be 10°C at 500 suns for terrestrial applications[9]. This implies a temperature drop of less than 1°C for our space module operating at 50 suns.

At this point in the assembly process, we have adhesive bonded cell stacks ready for inner lead bonding into TAB tape. Although inner lead bonding is a common process for IC's, there are several important distinctions associated with our tandem concentrator solar cell application. Our problem is simpler in its alignment and lead pitch aspects because each lead does not represent an isolated input or output signal. Unlike conventional IC's where bond pads are isolated from each other and recessed in a passivating layer, our bond pad configuration is a continuous planar film. This implies that 100% beam alignment and bond yield is not an absolute requirement for a functional, reliable interconnect. This also allows one to consider TAB bonding directly to the thin film metalization on the solar cell without forming the traditional bump common to TAB bonding. With bumpless bonding, special attention to the thickness of the thin film metalization is required to allow adequate mechanical compliance for the bonding process, and to achieve proper compositional control at the bond interface. The elimination of the bump offers a significant cost advantage as compared to conventional TAB. In our implementation, 5 mil leads on a 10 mil pitch are used to provide multiple interconnect redundancy, high current carrying capability, and thermal stress relief. This lead configuration is easily produced by either TAB tape suppliers or flex circuit manufacturers.

From a TAB assembly point of view, our problem appears complicated by the requirement to bond to the three separate planes presented by the front and back of the GaAs cell and the front of the GaSb cell. *Figure 7* shows a schematic of the tooling implemented to accommodate the separate bond planes. As shown in *Figure 7a*, a cell stack is placed on a die pedestal and secured with vacuum hold-down. This pedestal translates in the X, Y, and Z directions within a central square hole located in a tape carrier stage. The tape carrier stage has ramps shown schematically at the left and top of the central through hole to provide the required elevation differences for the beam leads relative to the back of the GaAs cell and the front of the GaSb cell. The tape is then secured to the stage through vacuum hold down outside of the leaded area. To position the cell stack relative to the three beam tape for bonding, a series of orthogonal motions are used between the stage and the pedestal. The first motion is illustrated in *Figure 7b*, and represents translation of the pedestal to the far right position, and up in the Z direction so that the back of the GaAs cell is at a higher elevation than the upper plane of the tape. The next motion is to translate the die pedestal back to the left and then down in the Z direction to allow the left beam lead set to lie underneath the bottom of the GaAs cell as shown in *Figure 7c*. A thermo-compression bonder is then used to gang bond the two beam lead sets to the top of the GaAs and GaSb cells. After these top side bonding operations are completed for all the sites in a TAB frame cassette or a tape reel, the cassette or reel is then turned over and the bottom GaAs beam lead set is gang bonded in a similar fashion as illustrated in *Figure 7d*.

The above inner-lead-bond (ILB) sequence has been implemented successfully using tin plated copper tape features bonded to either gold or silver thin film metalizations. It is believed that this process sequence can be implemented by a variety of commercial TAB equipment and represents a high throughput manufacturable ILB process. *Figure 8* shows a photograph of a tandem cell-stack in a three beam-lead-set TAB frame.

After inner lead bonding, the cell-stacks are tested for performance sorting. The cell-stack tape is then available for module assembly as shown in *Figure 3*. The operations involved in the cell-stack to module assembly are excising and beam lead forming, pick and place, die bonding, and outer lead bonding. As of this writing, we have not yet implemented these operations for production. However, these operations are nearly identical to standard automated assembly operations in use today in the semiconductor industry. Our efforts have been focused on the problems inherent in the

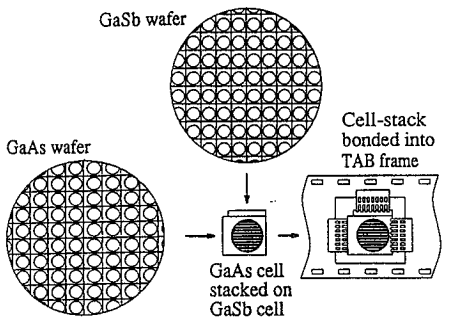

Fig. 4 Tape Automated Bonding of a cell-stack: a GaAs cell is first adhesive bonded to a GaSb cell and then inserted into a tape site for inner lead bonding.

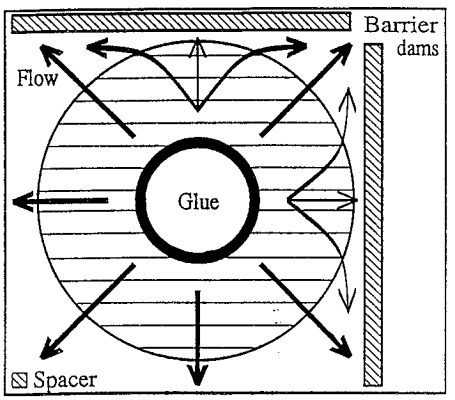

Fig. 5: The spacer and dam pattern on each GaSb chip provides electrical stand-off as well as a thin bond line for good thermal conductivity. The dams also serve to keep adhesive away from the lead bonding zones.

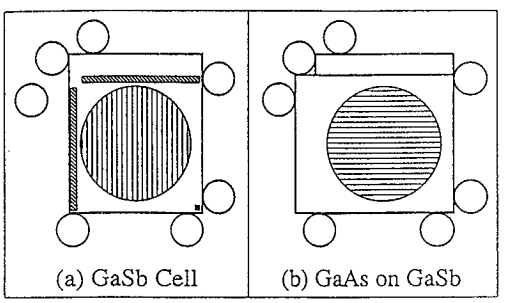

Fig. 6: The cell-stack pin alignment jig is used during adhesive bonding of the GaAs cell to the GaSb cell. The alignment fixture accommodates multiple stacking sites.

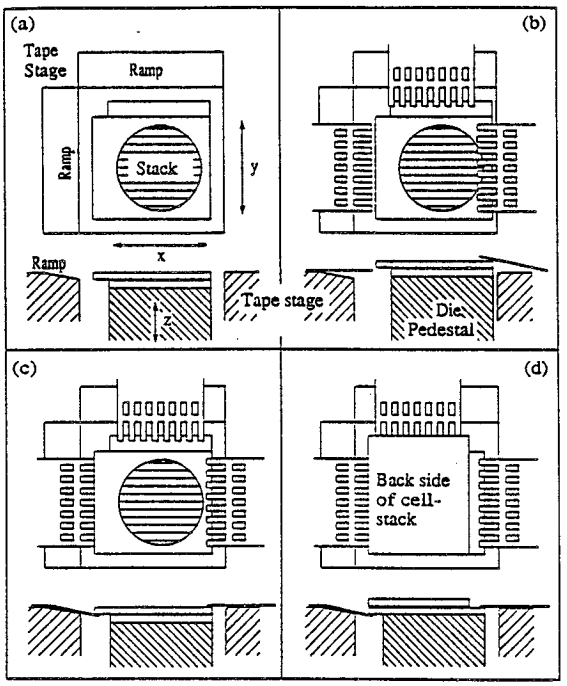

Fig. 7 3D TAB sequence is shown (a-d) for inner lead bonding of a cell-stack into a tape site. The cell-stack is mounted on a pedestal which is free to move within a square opening in the tape stage.

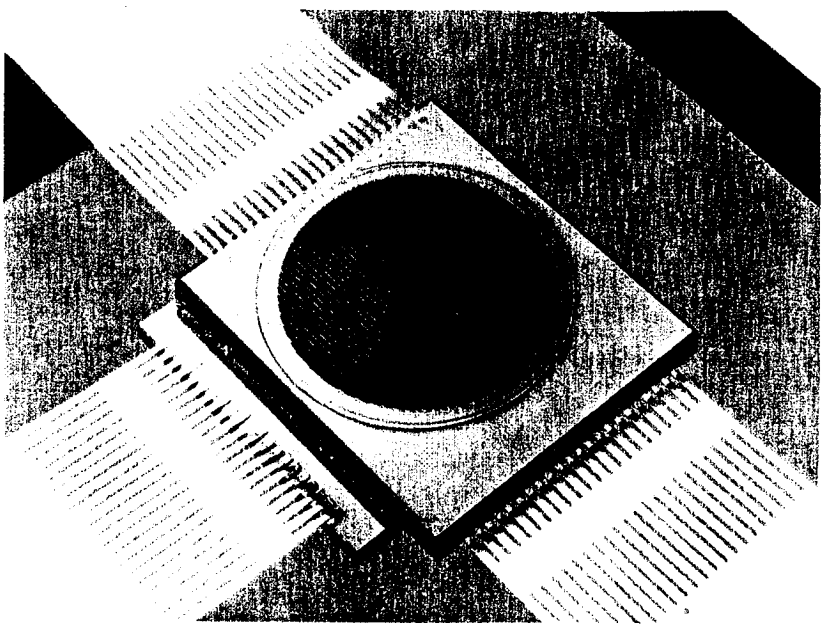

Fig. 8: A GaAs/GaSb cell-stack is shown inner lead bonded in a tape frame.

multi-planar tandem cell-stack. Once the cell-stack is inner lead bonded and tested in a TAB frame, it is no different than any other single chip in a TAB frame.

Concentrator Minimodule Assembly, Testing, and Performance

A. Minimodule assembly

In the previous section, we addressed the concentrator module assembly issues unique to the tandem cell-stack. In this section, we report the successful transfer of high cell efficiencies to high module efficiencies. The performance of a triplet minimodule is a particularly important demonstration of tandem cell technology integration at the module level. Cell stacks in a module are wired in groups of three, where the GaAs cells are connected in parallel and the GaSb cells are connected in series[6]. The triplets are two terminal devices that can be treated as if they were one solar cell with a bypass diode, and the triplet efficiency is a good indication of what the overall module efficiency will be.

Having established a cell-stack assembly process, module level assembly issues include connections between cell-stacks, heat removal, lens efficiencies, and optical alignment of components. Module testing involves analysis of the circuit performance at various temperatures, at various illumination levels with and without lenses in place, and module pointing tolerance. In addition to the fabrication and environmental testing of the PASP flight test module, we have decided to address module related issues by fabricating the rugged standard minimodules shown in *Figure 9*. These figures show both a single lens unit and a triplet. Each minimodule unit consists of two parts, a lens holder and a cell-stack housing. The lens holder fits precisely on the cell-stack housing to complete a standard assembly. A collimator assembly (not shown) replaces the lens holder on the single lens unit for lens efficiency measurements. These units serve three functions: 1) development and learning tools; 2) verification testing by outside laboratories; and 3) reference standard assemblies for calibrated performance testing of larger production modules.

The lens used in these units is the ENTECH minidome Fresnel lens described previously[10]. This silicone RTV lens is used as-molded without a protective glass dome or protective coating. Each square lens has an aperture area of 13.79 cm2. Typical optical efficiencies for these lenses range between 87% and 90%. This lens is designed to produce a 3 mm diameter spot on our cell. For a cell active area diameter of 5.6 mm, this provides an unilluminated guard band which leads to a tracking tolerance design of ± 2 degrees.

Most of our module measurements were obtained using a flash simulator system, shown schematically in *Figure 10*. The application of our flash simulator for cell circuit testing, lens testing and module testing has been described previously[11]. A new feature not described previously allowed for the quick acquisition of pointing tolerance data: the mirror shown has now been mounted on a robot arm so that its tilt can be programmed.

B. Tracking tolerance

Figure 11 shows the normalized current of a single lens standard assembly as a function of pointing angle. As predicted, the tolerance is ± 2 degrees. Also plotted is an example of how we were able to use a single lens standard as a learning tool for developing concentrator modules. Optical secondaries, used to relax the pointing tolerance of a concentrator module or array, have been described elsewhere for terrestrial applications[12]. In space applications, a solid optical secondary also serves as a radiation shield for the cell. By molding an optical secondary out of silicone (*Figure 12*) we were able, with minimal development, to experimentally demonstrate the increased tracking tolerance achievable with an optical secondary. As *Figure 11* shows, the pointing tolerance for our space concentrator unit can be increased from ± 2 degrees to ± 3.5 degrees.

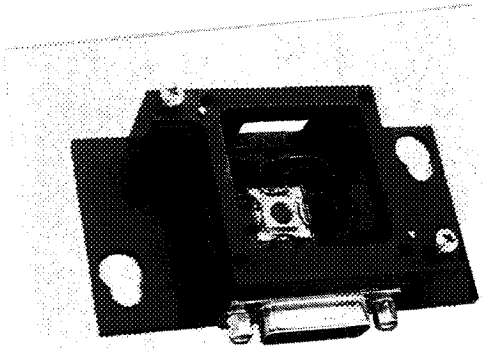

(9a) single cell-stack package

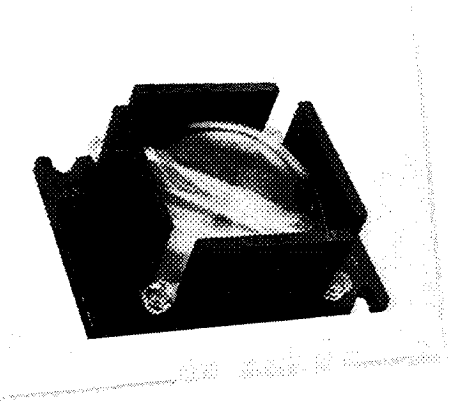

(9b) single lens holder

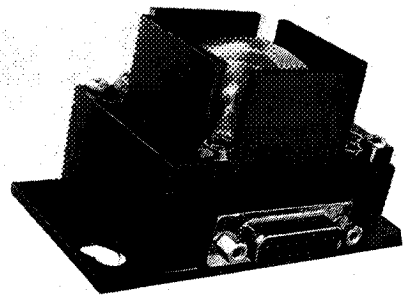

(9c) single lens-cell package

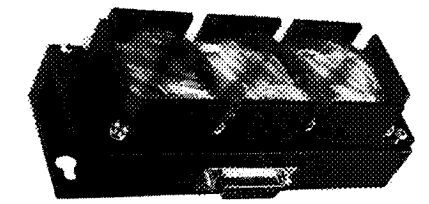

(9d) triplet lens-cell package

Fig. 9 The single and triplet tandem concentrator standard assemblies are shown (a-d). These rugged units are designed for calibration reference and performance verification. The "lens holder" (b) attaches to the "single cell-stack package" (a) to form the "single lens-cell package" (c).

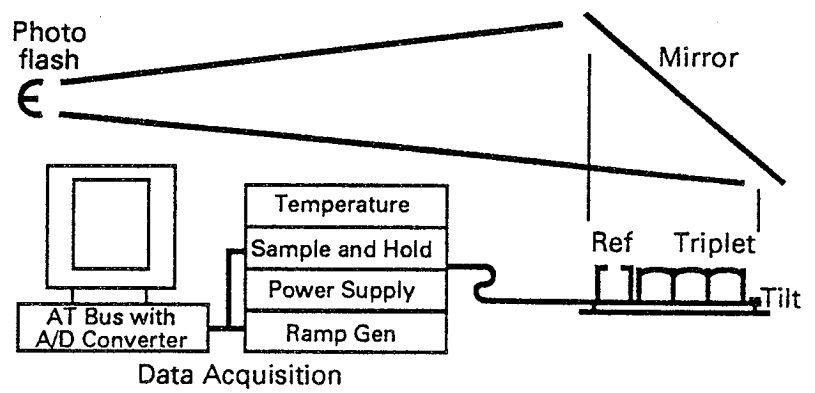

Figure 10. Flash Test Station for Measuring Concentrator Module Performance

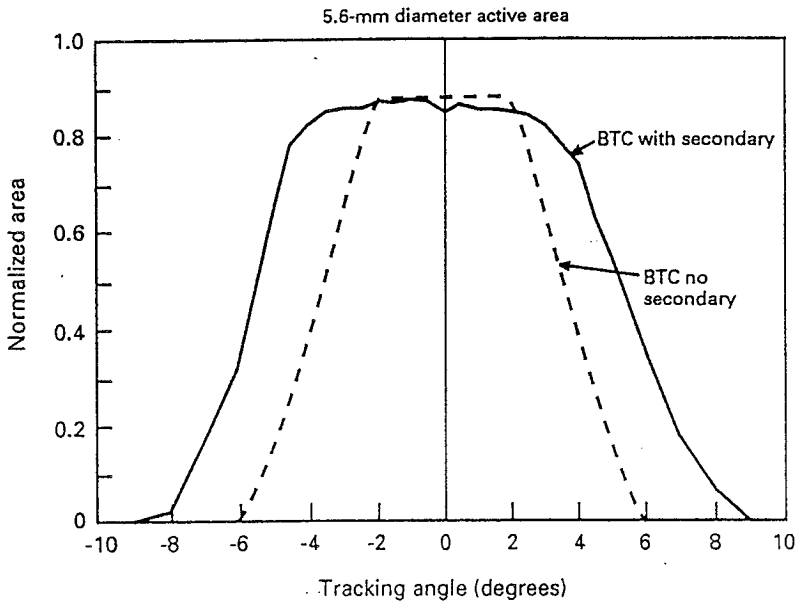

Fig. 11: The concentrator module off axis optical efficiency is shown with and without the optical secondary shown in figure 12.

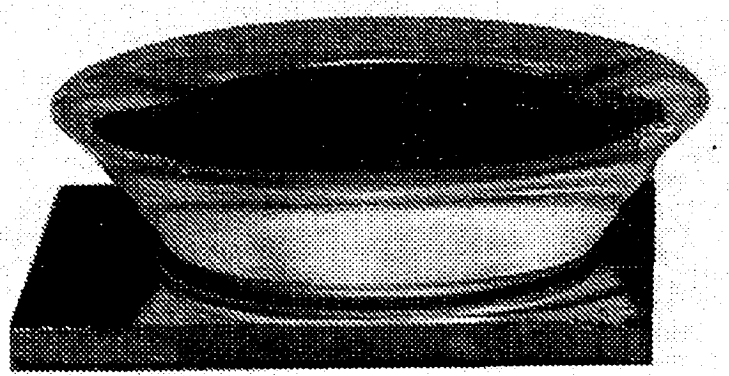

Fig. 12: Shaped cover slide for improved pointing tolerance.

	Efficiency	Fill Factor	Voc	Isc (mA)	Jsc (mA/cm2)
GaAs	**20.0%**	0.842	1.144	390	28.28
GaSb	**5.2%**	0.733	0.452	295	21.39
Combined	**25.2%**			3(GaAs)+1(GaSb):	[35.4]
Triplet	**25.0%**	0.842	1.160	1438	34.77
Notes: Single Lens Area = 13.79 cm2; Triplet Lens Area = 41.37cm2. Efficiencies reference, and Jsc are normalized to 1.36 kW/m2 insolation.					

Table 1: Lensed standard assembly performance.

C. Minimodule efficiency

We have now fabricated and tested high performance single lens and triplet minimodules. Table 1 summarizes the performance of these items (including lens losses) for space illumination conditions. The AM0 data shown in this table were obtained using our flash simulator. The flash lamp power level was first set to obtain the correct color ratio for the tandem stacked GaAs and GaSb cells. Then the lamp distance was adjusted to obtain the correct one-sun intensity using GaAs and GaSb standard cells that were calibrated to NASA Lear Jet flight standards. The minimodule power output is the maximum product of the measured I, V data pairs, e.g. 1.4 watts for the triplet under AM0. The power input is simply the illumination intensity times the total lens area, or 136 mW/cm2 x 13.79 cm2 x 3 = 5.6 watts for the triplet under AM0. The triplet AM0 efficiency is then 1.4 / 5.6 or 25%.

Conclusions

Mechanically-stacked concentrator GaAs/GaSb solar cells have achieved very high cell efficiencies, but have presented us with new challenges for module assembly. We have developed two separate procedures for assembling cell stacks: wire-bonding and TAB (bonding). Using wire-bonding and ceramic substrates, we have fabricated stacks for PASP and for high efficiency standard assemblies; however, this would be a difficult procedure to implement in large scale production. TAB technology is well established and easily scaled. We have demonstrated that it is feasible to bond together the two types of cells with a 8 μm thick glue line and then implement TAB techniques to make connections to three cell surfaces.
Lens/cell assemblies with 50X Entech domed Fresnel lenses were made in order to measure minimodule efficiencies. Using flash simulator testing and outdoor measurements, we have measured a triplet efficiency of 25.0% AM0 at 22°C.

Acknowledgments

The authors would like to acknowledge the assistance of Michael Fulton, Harold Soares, John Martin, Gene Fairbanks, Pat Gallagher and Bill Yerkes for antireflection coatings, cell-stack, PASP module and lens parquet assembly.

References

[1]N.R. Kaminar et al., 20th IEEE Photovoltaic Specialist Conference (PVSC) (1988): 766.
[2]S.P. Tobin et al., 21st IEEE PVSC (1990): 158.
[3]L.M. Fraas, P.E. Gruenbaum, et al., 22nd IEEE PVSC (1992): 80.
[4]P.E. Gruenbaum, L.M. Fraas, et al., *IEEE Trans. Electron Devices* (1992-this issue).
[5]L.M. Fraas, G.R. Girard, et. al., *J. Appl. Phys.* 66 (1989): 3866.
[6]L.M. Fraas, J.E. Avery, et. al., *IEEE Trans. Electron Devices*, ED-37 (1990): 443.
[7]L.M. Fraas and J.E. Avery, *Optoelectronics-Devices & Technol.*, 5 (1990): 297.
[8]M.F. Piszczor et al., 22nd IEEE PVSC (1992): 1485.
[9]J.M. Gee and C.J. Chiang, 21st IEEE PVSC (1990): 41.
[10]M.F. Piszczor et. al., 21st IEEE PVSC (1990): 1271.
[11]L.M. Fraas, J.E.Avery et. al, *ASME Solar Engineering 92* (1992): 825.
[12]M.S. Kuryla et al., 21st IEEE PVSC (1990): 1142.